Bioorganic & Medicinal Chemistry Letters 19 (2009) 3756–3759

Contents lists available at ScienceDirect

Bioorganic & Medicinal Chemistry Letters

journal homepage: www.elsevier.com/locate/bmcl

Identification of a disruptor of the MDM2-p53 protein–protein interaction facilitated by high-throughput in silico docking

Harshani R. Lawrence [a,b], Zhenyu Li [c], M. L. Richard Yip [b], Shen-Shu Sung [b], Nicholas J. Lawrence [a,d], Mark L. McLaughlin [a,d,e], Gregory J. McManus [e], Michael J. Zaworotko [e], Saïd M. Sebti [a,d], Jiandong Chen [c,d], Wayne C. Guida [a,b,d,e,*]

[a] Drug Discovery Department, H. Lee Moffitt Cancer Center and Research Institute, 12902 Magnolia Drive, Tampa, FL 33612, USA
[b] High-throughput Screening and Chemistry Core, H. Lee Moffitt Cancer Center and Research Institute, 12902 Magnolia Drive, Tampa, FL 33612, USA
[c] Molecular Oncology Department, H. Lee Moffitt Cancer Center and Research Institute, 12902 Magnolia Drive, Tampa, FL 33612, USA
[d] Department of Oncologic Sciences, University of South Florida, Tampa, FL 33620, USA
[e] Department of Chemistry, University of South Florida, Tampa, FL 33620, USA

ARTICLE INFO

Article history:
Received 24 February 2009
Revised 24 April 2009
Accepted 24 April 2009
Available online 3 May 2009

Keywords:
Virtual screening
Protein–protein interaction
Mdm2-p53
Anticancer
Alphascreen™

ABSTRACT

NSC 333003 has been identified from the NCI Diversity Set as an inhibitor of the MDM2-p53 protein–protein interaction by in silico docking (virtual screening). Its potency and chemical characteristics render it well suited for lead optimization studies that can result in more potent analogs with improved drug-like properties. Its synthesis was achieved using an acid catalyzed condensation reaction from commercially available benzothiazole hydrazine and pyridyl phenyl ketone in refluxing methanol. Stereochemical implications for this compound are described.

Protein–protein interactions play a prominent role in biological processes that are implicated in many diseases and, thus, are highly relevant targets for therapeutic intervention.[1] However, the design of novel drug-like small molecule inhibitors of protein–protein interactions represents an on-going challenge in current chemical biology.[2,3] In spite of the essentially infinite number of small molecules[4] that could be rationally designed or discovered via high-throughput screening for disruption of protein–protein interactions, obtaining such molecules (with some notable exceptions) has been extremely difficult.[5] Unlike enzyme or GPCR targets, that have generally yielded to the discovery and design of small molecule drugs, protein–protein interactions have been far more difficult targets mainly due to the large, shallow binding surfaces that are frequently involved.[5]

One such protein–protein interaction that is relevant for the discovery of novel therapeutic agents directed toward the treatment of cancer is the MDM2-p53 interaction. The tumor suppressor p53 is one of the most frequently altered proteins in human cancers.[6] It regulates cellular response to stress through a complex network of proteins known as the p53 pathway.[6] The MDM2 protein (the human form of which is frequently referred to as HDM2) is the principal negative regulator of p53 acting via two distinct mechanisms: (1) inhibition of wild-type (wt) p53 functions through direct binding thereby preventing p53 from binding to the transcriptional machinery; (2) targeting p53 for ubiquitination and degradation via the proteasome pathway by acting as a ubiquitin E3 ligase. Therefore, discovery of small molecules that can disrupt the MDM2-p53 interaction should increase the levels of p53 that trigger cell cycle arrest or apoptosis (programmed cell death), providing an attractive approach to treating tumors possessing wt-p53. In the recent years, a number of peptide inhibitors have been reported.[7] To overcome the pharmacokinetic shortcomings of peptides, the discovery of high potency non-peptidic small molecule inhibitors of the MDM2-p53 interaction has been pursued. In fact, proof-of-concept studies have demonstrated that small molecule inhibitors of MDM2-p53 interaction such as the nutlins[8], benzodiazepinones,[9] and spiro-oxindoles[10] in wt-p53 tumor cell lines represent a viable approach for cancer therapy. Rational structure-based design has also been used to design mimics of the p53 N-terminal alpha helix that binds MDM2.[11]

As a part of an on-going effort to identify new disruptors of the MDM2-p53 interaction for potential drug development, we performed in silico docking studies (virtual screening) of the National Cancer Institute compound databases.[12] Here we describe NSC 333003, a benzothiazole-hydrazone compound identified by

* Corresponding author. Tel.: +1 813 745 6047.
E-mail address: Wayne.Guida@moffitt.org (W.C. Guida).

0960-894X/$ - see front matter © 2009 Elsevier Ltd. All rights reserved.
doi:10.1016/j.bmcl.2009.04.124

virtual screening as a new inhibitor of the MDM2-p53 interaction and discuss its synthesis and the stereochemical implications involving the hydrazone moiety that could potentially affect binding to MDM2-p53.

NSC 333003 (**1**) is depicted in Figure 1. It is apparent that this small molecule can be easily modified for combinatorial library synthesis since it displays 3-points of chemical diversity: (1) the benzothiazole moiety; (2) the biaryl moiety; and (3) the hydrazone linker. Library design and synthesis can be focused on these functional units to potentially enhance the potency (Fig. 1a). Focused library synthesis can be easily carried out in a single step with commercially available benzophenone building blocks to obtain the final compounds. Therefore, NSC 333003 is an ideal scaffold for lead optimization.

The identification of NSC 333003 (**1**) via virtual screening and subsequent molecular modeling studies relied upon the X-ray crystal structure[9] of truncated human MDM2 in complex with an optimized p53 peptide at 1.90 Å resolution (PDB identification code: 1T4F). The alpha-helical optimized p53 peptide (residues 18–26) binds to a deep hydrophobic cleft within the amino-terminal domain of MDM2 and it was used to specify the dimensions of the MDM2 binding site for the docking studies. The binding site consists of a larger pocket for Phe-19 and Trp-23 of p53 and a smaller pocket for Leu-26 of p53, as shown in Figure 2. Both pockets are mainly hydrophobic.

Virtual screening was carried out using the GLIDE program (Grid Based Ligand Docking from Energetics, from Schrödinger, L.L.C.).[13,14] The Jorgensen OPLS-2001 force field is employed in the GLIDE program. The optimal binding geometry for each model was obtained with GLIDE, which relies upon Monte Carlo sampling techniques coupled with energy minimization. GLIDE uses a scoring method based on ChemScore but with additional terms added for greater accuracy. GLIDE 4.5 SP (Standard Precision mode) was used to dock the 3-D NCI Diversity Set[12] of 1990 compounds followed by GLIDE 4.5 XP (Extra Precision mode) docking of the top ranking compounds to find probable hits. Schrödinger's LigPrep was used to generate alternative tautomers, ring conformations, and ionization states, which initially increased the number of 3D structures from 1990 to 2967. Addition of enantiomeric pairs[15] increased this number to 3936.

After virtual screening, the top ranking 100 compounds based on their GLIDE XP generated docking scored (Gscores) were tested experimentally at 100 μM in an ELISA assay[16,17] which we used for the initial screening of the top ranking compounds contained in the NCI Diversity Set[12] supplied as 10 mM solutions in DMSO. One of these compounds, NSC 333003 (**1**) was found to be active (>50%

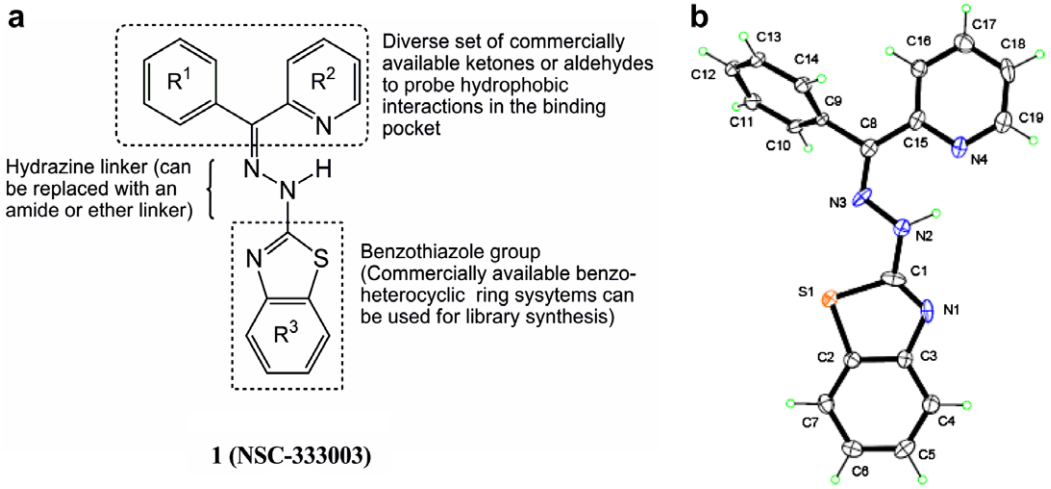

Figure 1. (a) Structural features of NSC 333003 for library synthesis (*Z*-isomer shown). (b) Structure of the major stereoisomer (*Z*-isomer) of NSC 333003 obtained by X-ray crystallography.

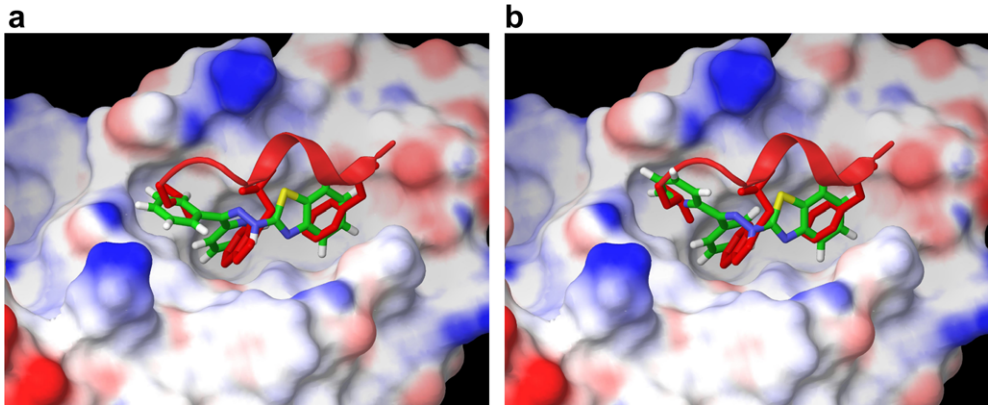

Figure 2. Computational model of NSC 333003 docked to the p53 binding domain of MDM2 shown by its molecular surface colored by electrostatic potential. Blue colored surface indicates positive electrostatic potential and red negative electrostatic potential. The p53 helical segment (shown in red) was included in this figure to compare the binding geometry of NSC 333003 to that of p53. The compound is colored according to atom types, carbon: green, nitrogen: blue, oxygen: red, sulfur: yellow and hydrogen: white. (a) Shows the *Z*-isomer and (b) shows the *E*-isomer.

inhibition at 100 μM) and dose response studies gave an IC_{50} of approximately 20 μM in the ELISA assay. Solid material was then obtained from the NCI and the activity of NSC 333003 was confirmed in an AlphaScreen™ assay[18,19] in which it exhibited an IC_{50} of 25 μM (Fig. 3). This assay is more appropriate for handling large numbers of samples and has been used in our subsequent screening with the ELISA assay employed as a confirmatory assay. The NCI material exhibited a ^{1}H NMR spectrum that was almost identical to the one we obtained for a sample synthesized in-house containing a putative 1:1 mixture of stereoisomers (vide infra).

The docked structures were further analyzed relative to the two stereoisomers of NSC 333003 (**1**), observed as the likely products of chemical synthesis (Fig. 2). The residues in the larger pocket in which residues Phe-19 and Trp-23 of p53 binds include Leu-54, Leu-57, Gly-58, Gln-59, Ile-61, Met-62, Tyr-67, Gln-71, Gln-72, His-73, Ile-74, Val-75, Phe-91, Val-93, and Ile-99. The residues in the smaller pocket in which residue Leu-26 of p53 binds include Leu-54, His-96, Ile-99, Tyr-100, and Ile-103, as shown in Figure 4. For the *Z*-isomer, the benzothiazole group and the pyridyl group are in the larger pocket and the phenyl group is in the smaller pocket. For the *E*-isomer, the benzothiazole group and the phenyl group are in the larger pocket and the pyridyl group is in the smaller pocket. The GLIDE XP docking scores (Gscores) for the *Z* and *E* isomers are −8.49 and −8.89 kcal/mol, respectively, favoring the *E*-isomer slightly, but the difference is not significant. The docking poses for the isomers are nearly identical with the benzene ring and pyridyl ring approximately swapping their positions; intramolecular hydrogen bonding is not observed.

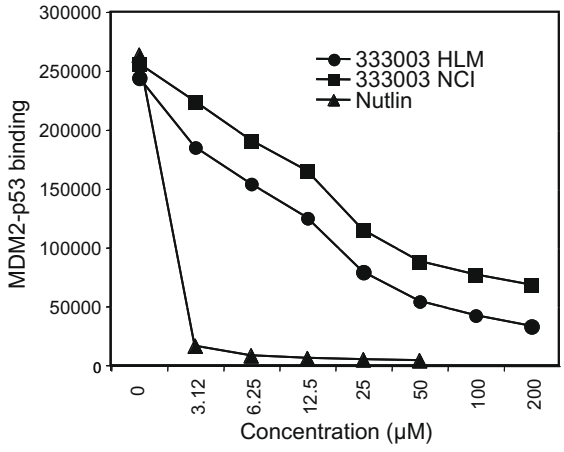

Figure 3. Dose–response curve for disruption of the MDM2-p53 interaction. NSC 333003 provided by the NCI or synthesized in-house (HLM) was tested in an AlphaScreen™ assay of GST-MDM2 binding to His6-p53. Nutlin-3a (literature[8] IC_{50} = 0.09 μM using surface plasmon resonance) was used as a control (the observed IC_{50} was 0.25 μM in our AlphaScreen™ assay).

The synthesis of NSC 333003 (**1**) was carried out in-house as only limited supplies of this compound were available from the NCI. The synthesis was useful to confirm the structure, purity and the biological activity. Synthesis of NSC 333003 was achieved via an acid catalyzed condensation reaction from commercially available benzothiazole hydrazine and pyridyl phenyl ketone in refluxing methanol for 8–12 h similar to a reported protocol.[20,21] However, the analytical data such as ^{1}H NMR, ^{13}C NMR, and mass spectrometry were not previously reported for this compound.[20] Column chromatography purified material was re-crystallized from boiling methanol to provide NSC 333003 as a 3:1 mixture of stereoisomers (as determined by ^{1}H NMR) in 26% yield. The observed inhibitory activity (IC_{50}) of this in-house sample (3:1 stereoisomer ratio) as determined by the AlphaScreen™ assay was 13 μM (Fig. 3). On standing at room temperature in DMSO-d_6 for 4–5 days, this mixture equilibrated to an approximately 1:1 mixture of stereoisomers by ^{1}H NMR analysis (t δ 7.94 and dt δ 7.88 changed from 1:3 to 1:1). The LCMS for the two samples were identical and, thus, decomposition of the compound was not observed in solution. Interestingly, this 1:1 mixture of stereoisomers exhibited the same IC_{50} by AlphaScreen™ (within experimental error, data not shown) as the unequilibrated material. Solution-phase equilibration of hydrazone stereoisomers is known and is apparently facile, especially in polar protic solvents such as ethanol.[22]

The crystal structure of NSC 333003 (**1**) obtained from the 3:1 mixture of stereoisomers was determined by single crystal X-ray diffraction and clearly showed the *Z*-configuration for the hydrazone moiety (Fig. 1b). However, a powder X-ray diffraction (PXRD) study on the bulk sample obtained from crystallization did not match the PXRD pattern calculated from the single crystal structure. Although this observation is consistent with a mixture of stereoisomers present in the solid phase bulk sample (as observed in solution by NMR) there are other possible explanations, including the presence of other crystal forms of the *Z*-isomer such as solvates or polymorphs.

There are a few reports of the biological activity of NSC 333003 (**1**). It has along with other pyridylhydrazones been reported to be cytotoxic against the P388 murine leukemia cell line.[20] Interestingly, NSC 333003 has been identified previously as a protein–protein interaction inhibitor. It targets an SH3 binding surface of the HIV type 1 Nef protein.[23] At this time, NSC 333003 has been screened in 57 assays as part of the Molecular Libraries Screening Center Network (MLSCN) and is active in only one.[24] In short, NSC

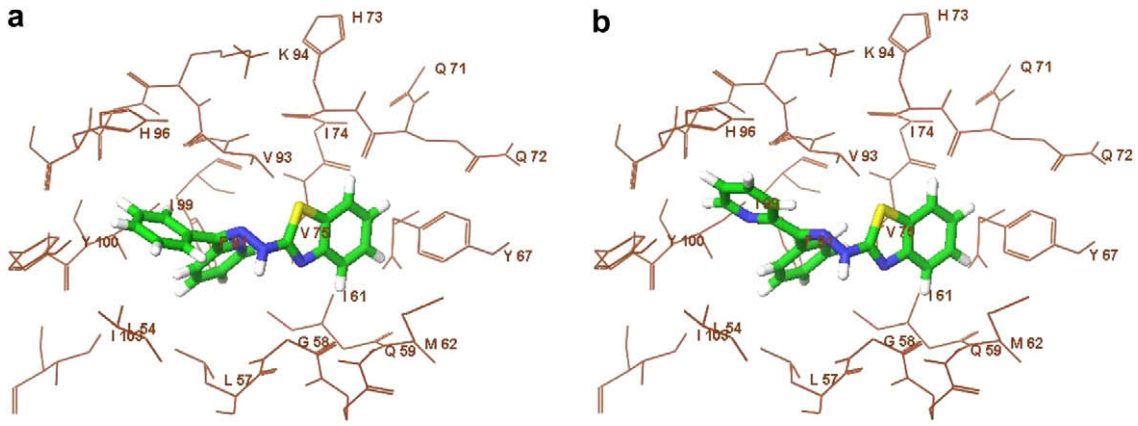

Figure 4. Residues of MDM2 at the NSC 333003 binding site. (a) *Z*-isomer and (b) *E*-isomer.

333003 appears to be devoid of indiscriminate and unselective biological activity.

In summary, a new disruptor of the MDM2-p53 interaction has been identified from the NCI Diversity Set by employing virtual screening of the entire set followed by experimental testing of only the top ranking compounds. From these 100 compounds, an active species was identified, NSC 333003 (**1**, Fig. 1), which is amenable to combinatorial library design. The ^{1}H NMR spectrum of this compound is consistent with a mixture of *E*/*Z* stereoisomers and an X-ray structure of the pure *Z*-isomer was obtained from single crystal diffraction of re-crystallized material. Although one might be tempted to speculate that the slightly different IC_{50} values we obtained for the solid material received from the NCI versus the material we synthesized in-house (25 μM vs 13 μM) are due to different *E*/*Z* stereoisomer ratios, it is more likely that this discrepancy is due to impurities in the sample obtained from the NCI. This conclusion is consistent with our observation that the in-house material that exhibited a 3:1 stereoisomeric ratio by NMR afforded an IC_{50} essentially identical to the equilibrated material that exhibited a 1:1 ratio of stereoisomers. Whereas the NCI material, which exhibited a 1:1 ratio of stereoisomers by NMR, gave a different IC_{50}. This conclusion is also consistent with the nearly identical docking scores we obtained for the *E* and *Z* stereoisomers and nearly identical docking poses we observed (Figs. 2 and 4). In any event, our ultimate goal is to replace the hydrazone moiety with more drug-like scaffolds and, indeed, ones that cannot readily isomerize. To that end, NSC 333003 can serve as a useful lead compound for the structure-based design of more potent drug-like analogs. Its potency (13 μM) is remarkable given that it has a relatively low molecular weight (330.41) and yet is capable of inhibiting a protein–protein interaction whose binding interface extends over approximately 900 Å^2.

Supplementary data

X-ray crystallographic data for **1** has been deposited with the Cambridge Crystallographic Data Centre (Deposition number CCDC 726777).

Acknowledgments

We are grateful to the National Institutes of Health for supporting this research through Grants P01CA118210 and P30 CA076292-10.

References and notes

1. Berg, T.; Cohen, B. S.; Desharnais, J.; Sonderegger, C.; Maslyar, J. D.; Goldberg, J.; Boger, D. L.; Vogt, K. P. *Proc. Natl. Acad. Sci. U.S.A.* **2002**, *99*, 3830; Ho, Y.; Gruhler, A.; Heilbut, A.; Bader, G. D.; Moore, L.; Adams, S. L.; Millar, A.; Taylor, P.; Bennett, K.; Boutilier, K.; Yang, L. Y.; Wolting, C.; Donaldson, I.; Schandorff, S.; Shewnarane, J.; Vo, M.; Taggart, J.; Goudreault, M.; Muskat, B.; Alfarano, C.; Dewar, D.; Lin, Z.; Michalickova, K.; Willems, A. R.; Sassi, H.; Nielson, P. A.; Rasmussen, K. J.; Anderson, J. R.; Johanson, L. E.; Hansen, L. H.; Jespersen, H.; Podtelejnikov, A.; Nielson, E.; Crawford, J.; Poulsen, V.; Sorenson, B. D.; Matthiesen, J.; Hendrickson, R. C.; Gleeson, F.; Pawson, T.; Moran, M. F.; Durocher, D.; Mann, M.; Hogue, C. W. V.; Figeys, D.; Tyers, M. *Nature* **2002**, *415*, 180; Veselovsky, A. V.; Ivanov, Y. D.; Ivanov, A. S.; Archakov, A. I.; Lewi, P.; Janssen, P. *J. Mol. Recognit.* **2002**, *15*, 405.
2. Berg, T. *Angew. Chem., Int. Ed.* **2003**, *42*, 462.
3. Yin, H.; Hamilton, A. D. *Angew. Chem., Int. Ed.* **2005**, *44*, 4130.
4. Bohacek, R. S.; McMartin, C.; Guida, W. C. *Med. Res. Rev.* **1996**, *16*, 3.
5. Wells, J. A.; McClendon, C. L. *Nature* **2007**, *450*, 1001.
6. Vassilev, L. T. *J. Med. Chem.* **2005**, *48*, 4491.
7. Hu, B.; Gilkes, D. M.; Chen, J. *Cancer Res.* **2007**, *67*, 8810; Garcia-Echeverria, C.; Chene, P.; Blommers, M. J. J.; Furet, P. *J. Med. Chem.* **2000**, *43*, 3205.
8. Vassilev, L. T.; Vu, B. T.; Graves, B.; Carvajal, D.; Podlaski, F.; Filipovic, Z.; Kong, N.; Kammlott, U.; Lukacs, C.; Klein, C.; Fotouhi, N.; Liu, E. A. *Science* **2004**, *303*, 844.
9. Grasberger, B. L.; Lu, T.; Schubert, C.; Parks, D. J.; Carver, T. E.; Koblish, H. K.; Cummings, M. D.; LaFrance, L. V.; Milkiewicz, K. L.; Calvo, R. R.; Maguire, D.; Lattanze, J.; Franks, C. F.; Zhao, S.; Ramachandren, K.; Bylebyl, G. R.; Zhang, M.; Manthey, C. L.; Petrella, E. C.; Pantoliano, M. W.; Deckman, I. C.; Spurlino, J. C.; Maroney, A. C.; Tomczuk, B. E.; Molloy, C. J.; Bone, R. F. *J. Med. Chem.* **2005**, *48*, 909.
10. Shangary, S.; Qin, D.; McEachern, D.; Liu, M.; Miller, R. S.; Qiu, S.; Nikolovska-Coleska, Z.; Ding, K.; Wang, G.; Chen, J.; Bernard, D.; Zhang, J.; Lu, Y.; Gu, Q.; Shah, R. B.; Pienta, K. J.; Ling, X.; Kang, S.; Guo, M.; Sun, Y.; Yang, D.; Wang, S. *Proc. Natl. Acad. Sci. U.S.A.* **2008**, *105*, 3933.
11. Yin, H.; Lee, G. I.; Park, H. S.; Payne, G. A.; Rodriguez, J. M.; Sebti, S. M.; Hamilton, A. D. *Angew. Chem., Int. Ed.* **2005**, *44*, 2704; Chen, L.; Yin, H.; Farooqi, B.; Sebti, S.; Hamilton, A. D.; Chen, J. *Mol. Cancer Ther.* **2005**, *4*, 1019.
12. National Cancer Institute, Developmental Therapeutics Program. http://dtp.nci.nih.gov/.
13. Friesner, R. A.; Banks, J. L.; Murphy, R. B.; Halgren, T. A.; Klicic, J. J.; Mainz, D. T.; Repasky, M. P.; Knoll, E. H.; Shelley, M.; Perry, J. K.; Shaw, D. E.; Francis, P.; Shenkin, P. S. *J. Med. Chem.* **2004**, *47*, 1739.
14. Halgren, T. A.; Murphy, R. B.; Friesner, R. A.; Beard, H. S.; Frye, L. L.; Pollard, W. T.; Banks, J. L. *J. Med. Chem.* **2004**, *47*, 1750.
15. Brooks, W. H.; Daniel, K. G.; Sung, S.-S.; Guida, W. C. *J. Chem. Inf. Model.* **2008**, *48*, 639.
16. Böttger, A.; Böttger, V.; Garcia-Echeverria, C.; Chène, P.; Heinz-Kurt Hochkeppel, H-K.; Sampson, W.; Ang, K.; Howard, S. F.; Picksley, S. M.; Lane, D. P. *J. Mol. Biol.* **1997**, *269*, 744; Böttger, A.; Böttger, V.; Sparks, A.; Liu, W. L.; Howard, S. F.; Lane, D. P. *Curr. Biol.* **1997**, *7*, 860.
17. *ELISA assay:* The procedure in Ref. 16 was followed. Briefly, His6-p53 was immobilized on 96-well ELISA plates. GST-MDM2 was then added in the absence or presence of potential inhibitors. GST-MDM2 bound to p53 was detected using MDM2 monoclonal antibody 5B10, followed by incubation with protein A-HRP conjugate and a chromogenic substrate.
18. The AlphaScreen™ assay, which is available from Perkin Elmer, relies upon donor and acceptor beads that are coated with hydrogel to provide functional groups for bioconjugation. When two proteins interact (one of which is conjugated to the donor bead and the other to the acceptor bead) the beads are brought into close proximity. Excitation of a photosensitizer in the donor bead results in the production of singlet oxygen that diffuses to and reacts with a chemiluminescent molecule in the acceptor bead. This results in the activation of fluorophores in the acceptor bead which results emitted light that can be detected.
19. *AlphaScreen™ assay:* GST-MDM2-1-150 and full-length His6-wt-p53 were expressed in E. coli and affinity purified under non-denaturing conditions. To detect the MDM2-p53 interaction by the AlphaScreen™ assay (Perkin Elmer), GST-MDM2-1-150 (30 nM), His6-p53 (30 nM), and potential inhibitors were mixed in a volume of 24 μl in binding buffer (PBS, 0.1% Tween 20, 10% glycerol) and incubated for 1 h at 24 °C. Nickel acceptor beads and glutathione donor beads were added (0.5 μg each) to reach a final volume of 30 μl. Following 1 h incubation at 24 °C, the mixture was analyzed in a fluorometer at an excitation wavelength of 680 nm. Nutlin-3a obtained from Cayman Chemical was used as a control. The IC_{50} values reported are from runs repeated four times.
20. Pellerano, C.; Savini, L.; Massarelli, P. *Farmaco. Ed. Sci.* **1985**, *40*, 645.
21. *Synthesis of NSC 333003:* A mixture of commercially available 2-benzoylpyridine (0.50 g, 2.70 mmol) and 2-hydrazinobenzothiazole (0.49 g, 2.97 mmol) in methanol (20 ml) containing 5 drops of glacial acetic acid was heated at 80 °C for 10–12 h. The reaction was followed by TLC (DCM/EtOAc 8:2 [R_f = 0.6] or EtOAc/hexane 3:7 [R_f = 0.3]) and TLC showed baseline impurities. The crude reaction mixture was evaporated and purified (SiO_2 flash chromatography, neat DCM). The purified material was re-crystallized from hot methanol and cooled to room temperature to obtain a pale yellow crystalline solid (0.33 g, 26%) as the required product. The X-ray crystal structure of the single crystal analyzed from the in-house material is shown in Figure 1b. Mp = 96–98 °C. The ^{1}H NMR of the re-crystallized compound was consistent with a 1:3 mixture of stereoisomers. ^{1}H NMR (DMSO-d_6, 400 MHz): δ 8.77 (br s, 1H), 8.44 (ddd, *J* = 4.8, 1.6, 0.8 Hz,1H), 8.14 (d, *J* = 8.0 Hz, 1H), 7.94 (br t, *J* = 7.6 Hz, 1H), 7.87 (dt, *J* = 8.0, 1.6 Hz, 1H), 7.70 (br s, 1H), 7.64 (d, 7.6 Hz, 1H), 7.50–7.49 (m, 4H), 7.43–7.21 (m, 10H), 7.28 (br t, 1H), 7.28–7.21 (m, 4H), 7.05 (br m, 3H); ^{13}C NMR (DMSO-d_6, 100 MHz): δ 163.9, 162.2, 150.3, 148.2, 147.6, 146.9, 145.2, 144.5, 143.5, 138.1, 133.0, 132.5, 131.7, 126.8, 126.6, 126.5, 125.0, 124.2, 124.1, 123.9, 121.5, 121.3, 121.1, 119.1, 118.8, 117.7, 116.8,116.6, 115.4, 115.4; ES-MS *m*/*z*: 331 (100, MH^+); ES-HRMS calcd for $C_{19}H_{15}N_4S$ (MH^+) 331.1011, found 331.1013, calcd for $C_{19}H_{14}N_4SNa$ ($M+Na^+$) 353.0831, found 353.0829.
22. Kwon, S.; Tanaka, M.; Isagawa, K. *Nippon Kagaku Kaishi* **1973**, 1314.
23. Betzi, S.; Restouin, A.; Opi, S.; Arold, S. T.; Parrot, I.; Guerlesquin, F.; Morelli, X.; Collette, Y. *Proc. Natl. Acad. Sci. U.S.A.* **2007**, *104*, 19256.
24. Huryn, D. M.; Cosford, N. D. P. *Ann. Rep. Med. Chem.* **2007**, *42*, 401.